Environment International 191 (2024) 108960

Contents lists available at ScienceDirect

Environment International

journal homepage: www.elsevier.com/locate/envint

Full length article

Reduced ovarian cholesterol and steroid biosynthesis along with increased inflammation are associated with high DEHP metabolite levels in human ovarian follicular fluids

Inge Varik [a], Runyu Zou [b], Andrea Bellavia [c], Kristine Rosenberg [a,d], Ylva Sjunnesson [e], Ida Hallberg [e,f], Jan Holte [g,h], Virissa Lenters [i], Majorie Van Duursen [i], Mikael Pedersen [j], Terje Svingen [j], Roel Vermeulen [b], Andres Salumets [k,l,m,n], Pauliina Damdimopoulou [k,m,#], Agne Velthut-Meikas [a,#,*]

[a] Department of Chemistry and Biotechnology, Tallinn University of Technology, Tallinn, Estonia
[b] Institute for Risk Assessment Sciences, Utrecht University, Utrecht, the Netherlands
[c] Department of Environmental Health, Harvard T.H. Chan School of Public Health, Boston, MA, USA
[d] Nova Vita Clinic, Tallinn, Estonia
[e] Department of Clinical Sciences, Division of Reproduction, The Center for Reproductive Biology in Uppsala, Swedish University of Agricultural Sciences, Uppsala, Sweden
[f] Department of Animal Biosciences, Division of Reproduction, The Center for Reproductive Biology in Uppsala, Swedish University of Agricultural Sciences, Uppsala, Sweden
[g] Department of Women's and Children's Health, Uppsala University, Uppsala, Sweden
[h] Carl von Linné Clinic, Uppsala, Sweden
[i] Amsterdam Institute for Life and Environment, Section Environmental Health and Toxicology, Vrije Universiteit Amsterdam, Amsterdam, the Netherlands
[j] National Food Institute, Technical University of Denmark, Kongens Lyngby, Denmark
[k] Department of Clinical Science, Intervention and Technology, Karolinska Institutet, Stockholm, Sweden
[l] Competence Center on Health Technologies, Tartu, Estonia
[m] Department of Gynaecology and Reproductive Medicine, Karolinska University Hospital, Huddinge, Sweden
[n] Department of Obstetrics and Gynaecology, Institute of Clinical Medicine, University of Tartu, Tartu, Estonia

ARTICLE INFO

Handling Editor: Shoji Nakayama

Keywords:
DEHP
Endocrine disrupting chemicals
Ovary
Follicular fluid
Reproductive health
Inflammation

ABSTRACT

The plasticizer di(2-ethylhexyl) phthalate (DEHP) is known to have endocrine-disrupting properties mediated by its many metabolites that form upon exposure in biological systems. In a previous study, we reported an inverse association between DEHP metabolites in the human ovarian follicular fluid (FF) and the responsiveness of the follicles to controlled ovarian stimulation during *in vitro* fertilization (IVF) treatments. Here, we explored this association further through molecular analysis of the ovarian FF samples.

Ninety-six IVF patients from Swedish (N = 48) and Estonian (N = 48) infertility clinics were selected from the previous cohort (N = 333) based on the molar sum of DEHP metabolites in their FF samples to arrive at "high" (mean 7.7 ± SD 2.3 nM, N = 48) and "low" (0.8 ± 0.4 nM, N = 48) exposure groups. Extracellular miRNA levels and concentrations of 15 steroid hormones were measured across FF samples. In addition, FF somatic cells, available for the Estonian patients, were used for RNA sequencing.

Differential expression (DE) and interactions between miRNA and mRNA networks revealed that the expression levels of genes in the cholesterol biosynthesis and steroidogenesis pathways were significantly decreased in the high compared to the low DEHP group. In addition, the DE miRNAs were predicted to target key enzymes within these pathways (FDR < 0.05). A decreased 17-OH-progesterone to progesterone ratio was observed in the FF of the high DEHP group ($p < 0.05$). Additionally, the expression levels of genes associated

Abbreviations: OSI, ovarian sensitivity index; IVF, *in vitro* fertilization; DEHP, di(2-ethylhexyl) phthalate; ASD, androstenedione; TES, testosterone; PRO, progesterone; HPR, 17-OH-hydroxyprogesterone; RNA-seq, RNA sequencing; FF, follicular fluid.

* Corresponding author at: Department of Chemistry and Biotechnology, Tallinn University of Technology, Akadeemia tee 15, 12618 Tallinn, Estonia.
E-mail address: Agne.Velthut@taltech.ee (A. Velthut-Meikas).
# These authors jointly supervised this work.

https://doi.org/10.1016/j.envint.2024.108960
Received 28 May 2024; Received in revised form 22 July 2024; Accepted 14 August 2024
Available online 15 August 2024

with inflammatory processes were elevated in the FF somatic cells, and a computational cell-type deconvolution analysis suggested an increased immune cell infiltration into the high DEHP follicles ($p < 0.05$).

In conclusion, elevated DEHP levels in FF were associated with a significantly altered follicular milieu within human ovaries, involving a pro-inflammatory environment and reduced cholesterol metabolism, including steroid synthesis. These results contribute to our understanding of the molecular mechanisms of female reprotoxic effects of DEHP.

1. Introduction

Endocrine disrupting chemicals (EDCs) can pose a risk to human health by interfering with the endocrine system by, for instance, disrupting hormone synthesis, transport, secretion, activity, and elimination (Schug et al., 2011). Among the many classes of chemicals harboring endocrine disrupting activities are phthalates, commonly used as plasticizers or additives in personal care products and cosmetics (David et al., 2012). Di(2-ethylhexyl) phthalate (DEHP), one of the most commonly used phthalates, has long been a component of various plastic products, including but not limited to food and beverage packaging, medical devices, toys, flooring, cosmetics, and personal care products (Koniecki et al., 2011). DEHP is known to leach from plastics due to its non-covalent association with polymers, and can enter the human body through ingestion, inhalation, or dermal absorption (Andersen et al., 2018; Schettler, 2006). Once in the body, DEHP undergoes rapid metabolism, resulting in the formation of metabolites such as mono(2-ethylhexyl) phthalate (MEHP), mono(2-ethyl-5-hydroxyhexyl) phthalate (MEHHP), mono(2-ethyl-5-oxohexyl) phthalate (MEOHP), and mono(2-ethyl-5-carboxypentyl) phthalate (MECPP). These metabolites are subsequently eliminated primarily through the urine (Koch et al., 2006). Despite being classified as a non-persistent chemical, the widespread presence of DEHP in everyday products with long half-lives causes continuous exposure to humans. Consequently, DEHP metabolites have been routinely detected in different human matrices, including urine, serum, breast milk, amniotic fluid, and follicular fluid (FF) (Bellavia et al., 2023; Frederiksen et al., 2010; Högberg et al., 2008; Katsikantami et al., 2020; Paoli et al., 2020).

The widespread use of, and exposure to, phthalates has raised concerns over potential adverse health effects, particularly on reproduction. For example, DEHP has been classified as an endocrine disruptor and toxic to reproduction by the European Chemicals Agency based primarily on data from males (European Chemicals Agency, 2024). There is, however, emerging evidence also suggesting effects on female reproductive health (Basso et al., 2022). For instance, DEHP can impact adult mouse ovarian health by inhibiting antral follicle growth, inducing follicle atresia, and disturbing steroidogenesis and granulosa cell proliferation (Hannon et al., 2023; Liu et al., 2021). Moreover, recent findings also suggests DEHP reducing the maturation and fertilization capacity of mouse oocytes through DNA damage and oxidative stress (Lu et al., 2019; Machtinger et al., 2018).

A limited number of human studies suggest an association between elevated DEHP levels and disrupted folliculogenesis, irrespective of exposure taking place during development or adulthood. The primary metabolite MEHP can induce the expression of genes controlling cholesterol and lipid synthesis in human fetal ovaries *in vitro*, potentially impacting ovarian development (Muczynski et al., 2012). Also, several epidemiological studies have demonstrated that high levels of DEHP metabolites in urine are linked to a significant decrease in antral follicle count, a lower number of mature and fertilized oocytes, and reduced quantity of top-quality embryos, suggesting that DEHP may impair *in vitro* fertilization (IVF) outcomes (Hauser et al., 2016; Messerlian et al., 2016). Coupled with our recent findings that increased concentrations of DEHP metabolites in FF are inversely correlated with the ovarian sensitivity index (OSI) – a measure of ovarian competence that links the dosage of recombinant follicle stimulating hormone (rFSH) to the number of retrieved oocytes in IVF treatment (Bellavia et al., 2023) – heightens the concern over the potential for DEHP to negatively impact human ovarian function. OSI is a major predictor of IVF treatment success and, although it also correlates with known ovarian reserve markers like anti-Müllerian hormone (AMH), it more accurately predicts live birth rates. This is likely because OSI provides a more functional measure of follicles than AMH levels (Revelli et al., 2020; Vaegter et al., 2019; Weghofer et al., 2020). Thus, our earlier findings imply that the functionality of the follicles may be modified by phthalates in the FF, potentially leading to a lower number of oocytes retrieved during IVF treatments.

Exactly how DEHP or its metabolites affect ovarian follicle growth in humans at the molecular level remains largely unknown. However, such evidence is needed to provide a causal link between initial chemical perturbation and adverse health outcomes. Such knowledge will also aid with developing better alternative test methods to assess female reproductive toxicity. To address this knowledge gap, we aimed to elucidate the molecular pathways by which DEHP metabolites may alter ovarian sensitivity. For this purpose, we generated RNA sequencing datasets from cell-free FF and the corresponding follicular somatic cells collected from IVF patients at infertility clinics in Sweden and Estonia. The patients were stratified into high and low DEHP groups based on previously measured DEHP metabolite levels in their FF. In addition, we assessed a panel of 15 steroid hormones from the same FF samples. By assessing the molecular signatures that differ between FF samples with high and low DEHP, a deeper understanding of how DEHP exposure may influence female fertility is gained.

2. Materials and methods

2.1. Ethical statement

The study was conducted in accordance with the Declaration of Helsinki. Both oral and written information was provided to the study participants after which they signed an informed consent form. Samples and data were pseudonymized with random codes and processed by relevant regulations (the Swedish data protection law PUL, the Swedish law on biobanking in healthcare, the European General Data Protection Regulation, and the Estonian Data Protection Act). The Swedish study was approved by the Swedish Ethical Review Authority (original license No. 2015/798–31/2, amendments 2016/360–32 and 2016/1523–32). The Estonian study was approved by the Research Ethics Committee of the University of Tartu (approval No. 356/M-4).

2.2. The patient cohort and previously measured variables

This study is based on the previously described merged cohort of 333 women recruited from Carl von Linnékliniken in Sweden and Nova Vita Clinic in Estonia (Bellavia et al., 2023). All patients underwent controlled ovarian stimulation (COST) and ovum pick-up procedure as described previously (Bellavia et al., 2023). Shortly, Swedish patients were stimulated according to the gonadotropin-releasing hormone (GnRH) agonist protocol (77 % of patients) using Suprecur (Cheplapharm Arzneimittel GmbH, Greifswald, Germany) or Synarela (Pfizer, New York City, New York, USA) where the pituitary was desensitized starting the luteal phase, or GnRH antagonist protocol (23 % of patients) where GnRH antagonist Orgalutran (N.V. Organon, Oss, The Netherlands) was given on day 6 of menses. rFSH (Gonal-F or Fostimon,

Bemfola, Gedeon Richter Plc., Budapest, Hungary) alone or with human menopausal gonadotropin (Menopur, Ferring Pharmaceuticals Ltd, Saint-Prex, Switzerland) were administered from day 3 of menses. Once ≥3 follicles with a diameter of ≥17 mm were detected, human chorionic gonadotropin (hCG) was given. After 36–37 h, oocytes were retrieved through the transvaginal ultrasound-guided ovarian puncture. For the Estonian patients, COST was conducted according to the GnRH antagonist (Cetrotide, Merck, Darmstadt, Germany) protocol with the administration of rFSH (Gonal-F®, Merck; Bemfola, Gedeon Richter Plc). All patients underwent oocyte retrieval 36 h after hCG injection (Ovitrelle®, Merck) if at least two follicles were observed with a diameter of ≥18 mm.

Once all cumulus-oocytes-complexes had been collected for the IVF procedure of the patient, the remaining FF was donated for research. Samples collected in Sweden (N = 48) contained FF from multiple follicles and were pooled for each patient, thereafter centrifugation was performed at 500 × g for 15 min. FF samples from the Estonian clinic (N = 48) were collected from a single leading follicle. The somatic cells from the follicular aspirate were pelleted by centrifugation at 300 × g for 10 min. Cell debris was removed from FF by an additional centrifugation at 2000 × g for 10 min. The cell-free FF samples were aliquoted and stored at −80 °C until further analysis. In addition, somatic cells were collected from the Estonian patients. Follicular cell pellets from the first round of centrifugation were lysed in 700 μL of QIAzol Lysis Reagent (QIAGEN, Hilden, Germany) and stored at −80 °C.

As described in our previous study, the concentrations of 59 EDCs were quantified in the FF samples using isotope dilution liquid chromatography with tandem mass spectrometry (LC-MS/MS) (Bellavia et al., 2023), and OSI was calculated for each patient according to the previously published formula(Huber et al., 2013): OSI = ln((number of oocytes retrieved)/(total rFSH dose (IU)) × 1000).

2.3. Selection of high and low DEHP samples for the present study

According to the power analyses described in the Supplementary Method, at least 90 participants are needed to achieve adequate statistical power for this study. Therefore, a sub cohort of 96 women from the original merged cohort of 333 women was selected based on the previously obtained concentrations of DEHP metabolites in the FF samples (Bellavia et al., 2023). Data on four DEHP metabolites, MEHP, MECPP, MEHHP, and MEOHP, were used. The concentrations for each compound were divided by their molar weight and summed to a variable referred to as ΣDEHP hereafter. Women were ranked by their ΣDEHP value, and samples were chosen from the top and bottom quartile with the following criteria: there should be equally many patients from Sweden and Estonia in both 1st and 4th ΣDEHP quartiles. To ensure comparability of two groups, we also considered the distribution of typical confounding factors in fertility studies: age, body-mass index (BMI), OSI, parity, and existence of experience with previous IVF cycles. The mean ΣDEHP concentration in the high and low groups (4th and 1st quartile, respectively) were 8 ± 2 nM (SD) and 0.9 ± 0.6 nM, respectively. The study design is depicted in Supplementary Fig. 1.

2.4. Quantification of steroids from follicular fluid

Steroid hormone levels were measured in selected FF samples by LC-MS/MS as previously described for plasma samples, with minor modifications (Draskau et al., 2019). All samples from Sweden (N = 48) were analyzed, while 23 and 17 samples from the low and high ΣDEHP groups, respectively, were available for analysis from the Estonian patients due to the more limited sample volume (Supplementary Fig. 1). A 100 μL of FF sample was added to a microcentrifuge tube containing 300 μL 2 % formic acid in acetonitrile with 3.33 ng/mL internal standard (deoxycortisol-d8 and cortisol-d4 from Cerilliant Corporation, Round Rock, TX, USA; methyltestosterone-d3, beta-testosterone-d2, beta-estradiol-d3 and progesterone-c2 from RIKILT, Wageningen, Netherlands), and then vortexed for 5 s. The vial was then placed in a freezer (−18 °C) for 20 min and centrifuged at 10,000 g for 7 min at 4 °C. The supernatant was subsequently transferred to a tube containing approximately 50 mg Supel™ QuE Z-Sep powder (Supelco, Bellefonte, PA, USA, #55418-U) and shaken for 60 s, before centrifugation for 3 min at 3,500 g. The supernatant was transferred to a centrifuge glass and dried using a nitrogen evaporator at 50 °C after which it was reconstituted in 50 μl acetonitrile, vortexed briefly, and mixed with 450 μl of MilliQ water.

Steroid hormones were separated, detected, and quantified using online-SPE LC-MS/MS using an Oasis HLB column (2.1 × 20 mm, 15 μm). For 17β-estradiol and estrone analysis, a Kinetex C18 column (2.1 × 100 mm, 2.6 μm) was used with an injection volume of 100 μl, measuring in negative ESI-mode using methanol, and 0.2 mM ammonium fluoride in water as the mobile phases (gradient flow rate was 0.4 mL/min). For the other hormones, an Ascentis Express C8 column (2.1 × 100 mm, 2.7 μm) was used with an injection volume of 100 μl, measuring in positive and negative ESI-mode with acetonitrile and 0.1 % formic acid in water as the mobile phases (gradient flow rate was 0.25 mL/min).

Fifteen hormones were assessed: aldosterone, testosterone (TES), epitestosterone, androstenedione (ASD), dehydroepiandrosterone (DHEA), dihydrotestosterone (DHT), corticosterone, cortisol, hydroxycortisol, deoxycortisol, pregnenolone, progesterone (PRO), 17a-OH-progesterone (HPR), beta-estradiol, and estrone. All hormones were detected, except for aldosterone, DHEA and DHT.

Limit of quantification (LOQ) was estimated as the concentration corresponding to 10 times the signal to noise ratio of FF spiked with analyte. LOQs were estimated to be 0.05 ng/mL for hydroxycortisol, 0.1 ng/mL for ASD, cortisol, PRO, TES, beta-estradiol and estrone, 0.2 ng/mL for deoxycortisol and epitestosterone, 0.3 ng/mL for corticosterone, HPR and aldosterone, 1.0 ng/mL for DHEA and DHT, and 2.0 ng/mL for pregnenolone. For quantification, external calibration standards were run before and after the samples at concentrations of 0.02, 0.05, 0.1, 0.2, 0.5, 1.0, 2.0, and 5.0 ng/mL, with 2.0 ng/mL internal standard. Blank FF were spiked with an analyte at three concentration levels: 0.0 (blank sample), 0.5, and 2.0 ng/mL and run for quality control. The mass spectrometer was an EVOQ Elite Triple Quadrupole Instrument from Bruker (Bremen, Germany) and the UPLC system was an Ultimate 3000 system with a DGP-3600RS dual-gradient pump. Data handling was performed with MS Workstation v. 8.2.1 software.

2.5. RNA extraction

The extraction of cell-free RNA from FF was performed with miRNeasy Micro kit (QIAGEN) with some modifications to the user manual. Shortly, 5 volumes of QIAzol Lysis Reagent (QIAGEN) was added to 500 μL of FF sample. After incubation, 500 μL chloroform and 5 μg of glycogen (Thermo Scientific) were added to the tube, followed by steps according to the miRNeasy Micro kit (QIAGEN) user manual. RNA concentration was measured using the Qubit small RNA assay kit on the Qubit 4.0 instrument (Thermo Fisher Scientific). All samples, 48 for low and 48 for high ΣDEHP group, were used (Supplementary Fig. 1).

RNA from FF somatic cells was extracted with miRNeasy Micro kit (QIAGEN) according to the kit protocol. The quality of RNA was assessed with the Bioanalyzer RNA 6000 Pico kit on Agilent 2100 Bioanalyzer instrument (Agilent Technologies, Waldbronn, Germany). RNA integrity number (RIN) > 7 was the accepted quality threshold for downstream analyses and 24 samples passed the threshold (13 and 11 samples in the high and low ΣDEHP groups, respectively) (Supplementary Fig. 1). RNA concentration was measured with the Qubit 4.0 instrument and Qubit RNA HS assay kit (Thermo Fisher Scientific).

2.6. Small RNA library preparation and sequencing

Small RNA libraries were prepared with QIAseq miRNA Library Kit (QIAGEN) according to the manufacturer's protocol. Libraries were

prepared from 5 μl of RNA extracted from FF samples. Final libraries were separated and excised from 5 % TBE gels (Bio-Rad Laboratories) after staining with 1X SYBR Gold stain (Thermo Fisher Scientific). Gel pieces containing the small RNA libraries were crushed with pellet pestles (Fisher Scientific). Then, 300 μL of RNase free water (Thermo Fisher Scientific) was added to the gel debris and the tubes were rotated for 2 h at room temperature to elute miRNA libraries. Eluate and gel debris were transferred to the Spin X centrifuge tube filter (Merck, Darmstadt, Germany) and centrifuged for 2 min at 16,000 g. Thereafter 10 μg of glycogen (Thermo Fisher Scientific), 30 μL 3 M NaOAc (Thermo Fisher Scientific), 1 μL 0.1X Pellet Paint (Merck) and 975 μL of cold 100 % ethanol (Naxo, Tartu, Estonia) were added to the eluate, and centrifuged for 20 min at 20,000 g at 4 °C. Pellet was washed with 500 μL of 70 % ethanol and centrifuged for 2 min at 20,000 g. The final libraries were resuspended in 7 μL of Resuspension buffer (PerkinElmer, Massachusetts, USA). The size of the libraries was estimated with Agilent DNA High Sensitivity chips on the Agilent 2100 Bioanalyzer system (Agilent Technologies). Library concentrations were measured using Qubit High Sensitivity DNA Assay kit (Thermo Fisher Scientific) before pooling in equimolar amounts. Single-end sequencing of 76 bp length was performed on NextSeq 500 platform with NextSeq 500/550 High Output Kit v2.5 (Illumina, San Diego, CA, USA) with 32 libraries per flow cell.

2.7. mRNA library preparation and sequencing

RNA with sufficient quality and concentration was available for 24 Estonian samples (N = 13 in the high ΣDEHP and N = 11 in the low ΣDEHP group) (Supplementary Fig. 1). Libraries of RNA extracted from FF somatic cells were prepared according to the Smart-seq2 protocol (Picelli et al., 2014) with small modifications. Ten ng of total RNA was used for cDNA synthesis and ten cycles of PCR for pre-amplification, instead of using single cells as described by the original Smart-seq2 protocol. KAPA HiFi DNA polymerase was replaced with Phusion High-Fidelity DNA Polymerase (Thermo Scientific) compatible with the original protocol. The protocol selects for polyadenylated RNA molecules and provides full coverage. The size and concentration of the final libraries were measured as described above for small RNA sequencing. Single-end sequencing of 122 bp length was performed on NextSeq 2000 platform on the P2 flow cell with NextSeq2000 P2 100 cycles kit (Illumina, San Diego, CA, USA).

2.8. Small RNA-seq data analysis

The raw data analysis was performed in the My QIAGEN GeneGlobe environment using the QIAseq miRNA Library Kit analysis workflow (QIAGEN). Briefly, the raw reads were trimmed of adapter sequences, quality-filtered and sequences with identical unique molecular identifiers were collapsed. The remaining reads of 15–55 nucleotides in length were annotated according to the miRBase v22 (Kozomara et al., 2019). The list of unique molecular counts of each miRNA was used as input for differential expression (DE) analysis in DESeq2 v1.40.2 (Love et al., 2014) in R v4.3.1 (R Core Team, 2023). MiRNAs expressed at low levels, determined as below 2 counts per million (cpm) in <25 % of samples were removed from the analysis.

Principal component analysis (PCA) was performed within the DESeq2 package for all detected miRNAs (N = 465). Variance stabilizing transformation was performed with option blind = FALSE for the normalized count table before drawing the PCA plot. Because PCA detected 3 outliers, 93 samples were ultimately included in the miRNA analysis. The country of origin (i.e. Sweden or Estonia) was used as a covariate in all DE analyses. The statistical significance cut-off for differentially expressed (DE) miRNAs in DESeq2 analysis was set at Benjamini-Hochberg (BH) false discovery rate (FDR) <0.1.

For predicting mRNA targets for the DE miRNAs, miRWalk (Sticht et al., 2018) prediction tool was used. Only genes with target sites in their 3́UTR mRNA region with a binding score of 1 are reported.

In addition, the list of statistically significant DE miRNAs was used as input to miRNA Enrichment Analysis and Annotation Tool (miEAA), which performs miRNA target prediction and over-representation analysis of gene ontology terms simultaneously by combining linked external databases (Aparicio-Puerta et al., 2023). Over-representation analysis was performed for WikiPathways (Agrawal et al., 2024) via miRPathDB (Kehl et al., 2020). Pathways targeted by ≥3 miRNAs with BH FDR < 0.05 are reported. The network between miRNAs and their targeted pathways was visualized in Cytoscape v3.9.1 (Shannon et al., 2003).

2.9. mRNA-seq data analysis

Raw FASTQ files were quality filtered using Trimmomatic v0.39 with the options LEADING:3 SLIDINGWINDOW:3:20 (Bolger et al., 2014). Reads below 36 nucleotides in length were discarded and all adapter sequences provided by Illumina were removed from the reads. The remaining reads were aligned to the primary assembly of human genome GRCh38 retrieved from GENCODE using STAR aligner v2.7.1 with standard settings (Dobin et al., 2013). Annotation of reads to genes was performed with htseq-count algorithm (Anders et al., 2015) (HTSeq v 0.11.2, Python v3.6.4) by using the primary assembly annotation GTF file v104 from Ensembl. The intersection nonempty option was used in htseq-count for annotating reads that overlapped with multiple features.

The count file produced by htseq-counts was used as input for DeSeq2 for DE analysis between high and low ΣDEHP groups with standard options. Genes expressed at low levels (<10 cpm across 50 % of samples) were removed from the analysis. The statistical significance cut-off for DE mRNAs in DESeq2 analysis was set at BH FDR <0.05. Volcano plot was created with the R package EnhancedVolcano v1.22.0.

The enrichment of DE genes in Reactome pathways was analyzed by g:Profiler (Kolberg et al., 2023) and results with BH FDR <0.05 are reported. The enriched pathways were visualized using publicly available web application ShinyGO (Ge et al., 2020).

2.10. Cell-type deconvolution analysis

CIBERSORTx (Newman et al., 2019) was used to estimate the proportion of different cell types in the FF somatic cell pool used in RNA-seq. To predict the cell types, we used our previously published single cell RNA-seq dataset describing cell types in human ovarian follicles as a reference (Roos et al., 2022). Importantly, the stimulation and sample collection protocols for the single-cell RNA-seq study (Roos et al., 2022) matched those of the current study as the patients were recruited from the same infertility clinic. A signature single-cell expression matrix of each cell type was generated with S-batch correction. The permutation value was set to 100. The relative abundance of cell type fractions was calculated as an average of three runs. Cell type proportion differences between the high and low ΣDEHP groups were compared using the Student's *t*-test.

2.11. Statistical analysis

Mann-Whitney *U* test was used to analyze the differences in patient baseline characteristics for continuous variables and chi-squared test was used for categorical variables. Spearman correlation was used to determine associations between ΣDEHP and other EDCs with $p < 0.05$ suggesting statistical significance. In case of Mann-Whitney U tests and correlation analyses, the statistical significance is noted in figures as follows: * $p < 0.05$, ** $p < 0.01$, *** $p < 0.001$. For all genome-wide sequencing analyses, the statistical significance of the results has been corrected for multiple testing by using the BH FDR and the cut-off (FDR < 0.1 or FDR < 0.05) has been specified for each analysis.

3. Results

3.1. Description of patients and ΣDEHP groups

IVF patients from Sweden and Estonia were recruited to study the links between FF EDCs and the outcomes of infertility treatment. The analysis of 59 EDCs in FF and their associations with OSI in the merged cohort of 333 women were reported previously (Bellavia et al., 2023). Here, a sub cohort of these women was analyzed further to reveal molecular alterations underlying the negative association between ΣDEHP and ovarian function.

The FF samples were selected for the molecular analysis based on their concentrations of ΣDEHP while keeping confounders similar. The low ΣDEHP group was composed of samples from the 1st and high ΣDEHP group from the 4th quartile of measured concentrations, without any overlap, resulting in a high statistical significance of the concentration differences ($p < 0.001$, Table 1 and Supplementary Fig. 2A). Patients from both countries were equally represented ($N = 48 + 48$). Attention was given to maintaining comparable average OSI across the patient groups, ensuring the ability to draw conclusions about the impact of ΣDEHP on the ovarian microenvironment, uninfluenced by ovarian sensitivity (Table 1 and Supplementary Fig. 2B). In addition, general patient characteristics, were evenly distributed between two groups (Table 1), including typical confounding factors in fertility studies (BMI, age, parity, and previous IVF treatments).

Exposure to mixtures of EDCs is widespread, and the exposure levels may vary among individuals due to factors like the local use of chemicals, lifestyle, diet, age, and parity. Consequently, the concentrations of other EDCs, apart from ΣDEHP, may also differ between the patients in our study. Therefore, we analyzed correlations between ΣDEHP and the other previously measured EDCs (Bellavia et al., 2023). We found country-specific differences in correlations between chemicals: namely, ΣDEHP concentrations demonstrated a statistically significant positive correlation ($p < 0.05$) with methylparaben and PFHxS only in the Estonian women, while MEP and cxMiNP correlated with ΣDEHP in the combined cohort (Table 2). As these chemicals may possess independent molecular effects on ovarian function, we have normalized all subsequent analyses to the country of sample origin.

3.2. ΣDEHP levels correlate with altered FF miRNA profile

We aimed to analyze miRNAs in the FF, the liquid that makes up most of the volume of the preovulatory follicle, because of the suggested role of miRNAs in intercellular signaling (Valadi et al., 2007). Among the 465 miRNAs present in ≥25 % of the samples with expression level of ≥2 cpm, the country of origin explained most of the variance of miRNA expression ($p = 1.768*10^{-11}$ of the difference between PCA scores), while the ΣDEHP group separated the samples across the second principal component ($p = 0.0077$, Fig. 1A and Supplementary Fig. 3). This result again justified the use of the country of origin as a covariate in downstream DE analyses.

In total, 16 miRNAs were differentially expressed between the high and low ΣDEHP groups (FDR < 0.1) with the most robust differences observed for hsa-miR-203a-3p (FDR = 0.0001), hsa-miR-150-5p (FDR = 0.0382) and hsa-miR-28-3p (FDR = 0.0410) that were all more abundantly expressed in the high ΣDEHP group (Fig. 1B and Supplementary Table 1). To understand their potential function in the ovary, the target genes for the DE miRNAs were predicted and their interactions with signaling pathways were modeled. We identified 51,697 regions in total in the human transcriptome targeted by the 16 DE miRNAs (Supplementary Table 2). This high number is not surprising as multiple mRNA isoforms may be transcribed from one gene, and each transcript isoform may have multiple predicted miRNA target sites. The identified targets represented 10,998 unique genes. We aimed to understand which signaling pathways are potentially co-targeted by multiple DE miRNAs, and carried out a gene enrichment analysis together with miRNA target prediction. Adipogenesis, RAC1/PAK1/p38/MMP2, androgen receptor (AR) signaling, and AGE/RAGE pathways were each targeted by ≥ 5 DE miRNAs (FDR < 0.05, Fig. 1C). Three different pathways involving the Bone Morphogenetic Protein (BMP) signaling are targeted by 3 miRNAs each (FDR < 0.05, Supplementary Table 3).

Next, we examined if any of the DE miRNAs correlate with OSI that may explain the negative association between ΣDEHP concentration and OSI reported in our previous study[10]. Indeed, the most up-regulated miRNA in the high ΣDEHP group, hsa-miR-203a-3p, correlated negatively with OSI (age-adjusted $R = -0.27$, $p < 0.05$, Fig. 1D). None of the other DE miRNA showed statistically significant correlations.

Table 1
Descriptive statistics of study groups.

Characteristic	Low ΣDEHP (N = 48)	High ΣDEHP (N = 48)	p-value
Age (years)	34.8 (4.2)	33.6 (4.7)	0.19
BMI (kg/m2)	22.4 (3.2)	23.8 (3.4)	0.05
OSI	0.6 (0.4)	0.7 (0.4)	0.51
∑DEHP (nM)	0.9 (0.6)	8 (2)	<0.001
Parity (≥1)	24 (50 %)	20 (42 %)	0.54
Previous IVF treatment (Yes)	20 (42 %)	21 (44 %)	0.84

Statistics are presented in mean (SD) or number (percentage); *t*-test, Mann–Whitney *U* test, or chi-square test was performed for between-group comparison. Abbreviations: ΣDEHP, sum of di(2-ethylhexyl) phthalate metabolites; BMI, body mass index; OSI, ovarian sensitivity index; IVF, *in vitro* fertilization.

3.3. Gene expression changes in follicular fluid cells indicate ΣDEHP-linked disturbances in the immune system and steroidogenesis pathways

The FF somatic cells consist mainly of mural granulosa cells (Roos et al., 2022) responsible for producing steroid hormones necessary for the feedback within the hypothalamus-pituitary-ovarian axis and endometrial maturation. Our samples were collected after the hCG trigger, which initiates the luteinization of the cells and switches the steroid production from estradiol to PRO. While extracellular miRNAs may be involved in modulating gene expression in the cells, ΣDEHP in FF could also directly influence the functionality and differentiation of the somatic cells.

To understand the overall effect of ΣDEHP to the cellular gene expression in the preovulatory follicle, we carried out RNA-seq from the follicular somatic cells corresponding to the same FF samples analyzed for ΣDEHP concentration and miRNA levels. Such cellular samples were available for a subset of the Estonian patients (Supplementary Fig. 1).

We detected 14,820 genes expressed at ≥ 10 cpm in ≥ 50 % of samples, out of which 2,454 were DE between the high and low ΣDEHP groups (FDR < 0.05, Fig. 2A, Supplementary Table 4). We carried out signaling pathway enrichment analyses to understand what processes were upregulated in the presence of high or low ΣDEHP, and found striking differences. Follicles with high ΣDEHP showed enrichment in processes related to immune system pathways (Fig. 2B, Supplementary Table 5). In contrast, follicles with low ΣDEHP demonstrated enrichment of different metabolic processes: for instance, cholesterol biosynthesis as well as lipid and steroid hormone metabolism were among the top 10 enriched Reactome pathways. In addition, follicles with low ΣDEHP showed enrichment in pathways involving mitochondria: tricarboxylic acid (TCA) cycle, gluconeogenesis, respiratory electron transport, and mitochondrial translation (Fig. 2C, Supplementary Table 6), meaning that these crucial metabolic pathways were down-regulated in follicles containing high ΣDEHP.

Cytokine signaling is an important mechanism of cellular communication in the ovarian follicle. However, the upregulated immune system pathways in the high ΣDEHP group may also indicate a disproportionate number of leukocytes among the somatic cell pool. To study this further, we performed a cell population deconvolution

Table 2
Spearman correlation between the molar concentration of ΣDEHP and concentrations of other endocrine-disrupting chemicals detected in >90 % of subjects (N = 96).

Cohort		MEP	cxMiNP	MOHiBP	MePAR	PFHxS	PFOA	PFOS	PFNA	PFDA	PFunDA	Sum[#]
All	ΣDEHP	0.22*	0.40*	0.15	0.04	0.15	0.18	0.12	0.16	0.16	0.09	0.13
Swedish		0.31*	0.21	0.10	−0.19	−0.11	0.19	−0.09	0.12	0.10	0.11	−0.01
Estonian		0.07	0.62*	0.19	0.48*	0.36*	0.17	0.24	0.11	0.16	0.001	0.51*

* $p < 0.05$.
[#] Sum refers to the sum of molar concentrations of all chemicals except ΣDEHP. Abbreviations: MEP, monoethyl phthalate; cxMiNP, mono-(4-methyl-7-carboxyheptyl)phthalate; MOHiBP, mono(2-hydroxyisobutyl)phthalate; MePAR, methyl paraben; PFHxS, perfluoro-1-hexanesulfonate; PFOA, perfluoro-n-octanoic acid; PFOS, perfluoro-octanesulfonate (sum); PFNA, perfluoro-n-nonanoic acid; PFDA, perfluoro-n-decanoic acid; PFunDA, perfluoro-n-undecanoic acid.

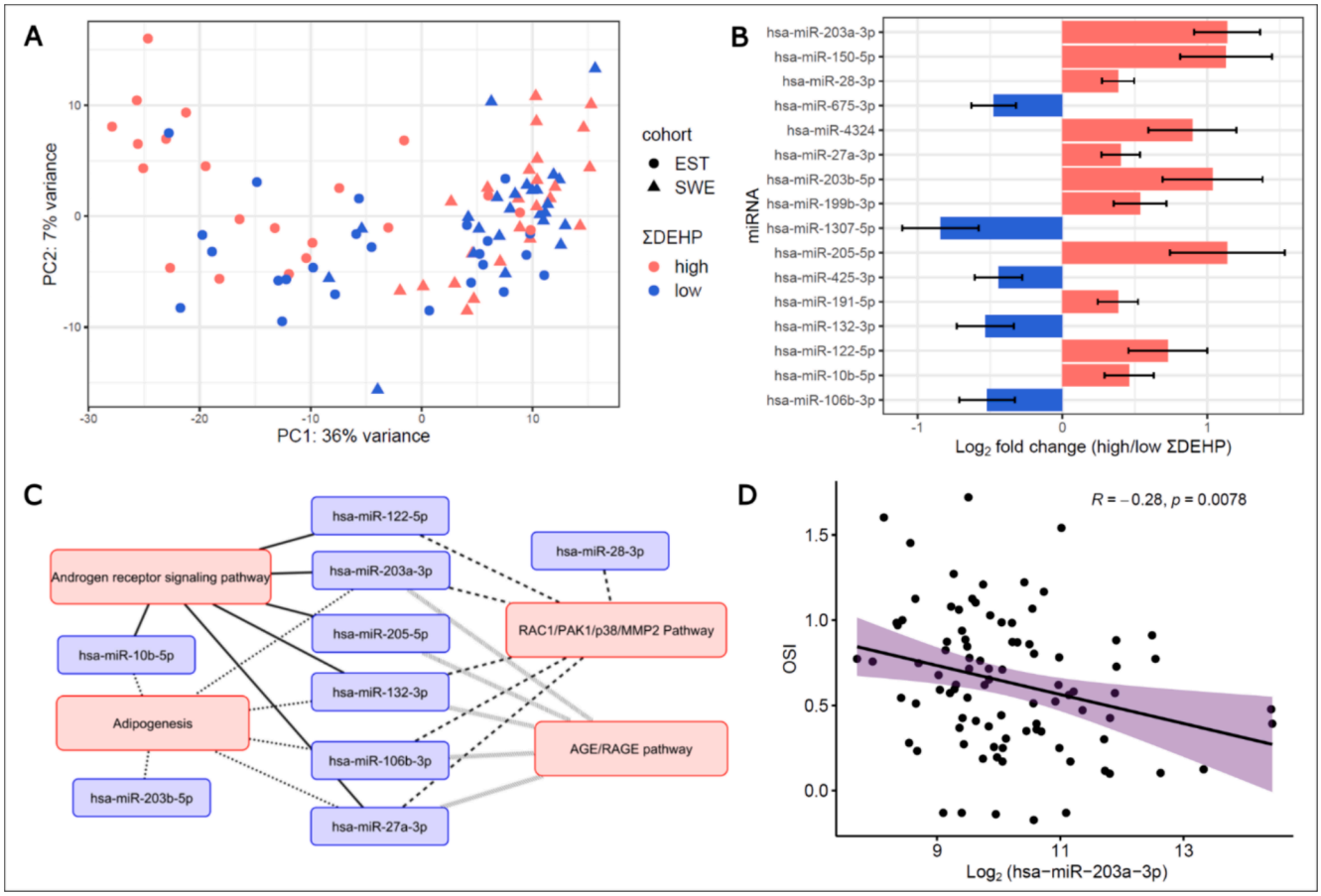

Fig. 1. Differential expression of miRNAs between high vs low ΣDEHP groups. A: Principal component (PC) analysis segregating the analyzed samples according to the expression of 465 detected miRNAs. B: Differentially expressed (DE) miRNAs between high vs low ΣDEHP group (FDR < 0.1). C: Interaction map of DE miRNAs and their targeted molecular pathways. Only pathways targeted by ≥ 5 DE miRNAs (FDR < 0.05) are presented. Each line type links miRNAs to a specific pathway. D: Negative correlation between the expression of miRNA hsa-miR-203a-3p and ovarian sensitivity index (OSI).

analysis by merging the current bulk mRNA sequencing data with our previous single-cell RNA-seq data on FF cells from fertile women with normal ovarian response to COST (Roos et al., 2022). Interesting findings were observed for the leukocyte proportions: the marker genes for T-cells, M1 and M2 macrophages as well as neutrophils were all expressed at increased levels in the high ΣDEHP group suggesting higher proportions of these cell types in the follicle ($p < 0.05$ for neutrophils and $p < 0.01$ for other leukocytes, Fig. 2D). At the same time, the analysis results suggested a reduced proportion of granulosa cells in the samples ($p < 0.001$) (Fig. 2D).

3.4. Coding and non-coding gene expression differences associated with ΣDEHP concentrations interfere with the cholesterol metabolism and steroidogenesis pathways

As the genes involved in cholesterol biosynthesis and steroidogenesis pathways were the most robustly down-regulated in the high ΣDEHP group (Supplementary Table 6), we aimed to further focus on the miRNA:mRNA interactions in these pathways.

Cholesterol is the precursor molecule for the steroid hormones produced by the somatic cell populations in the follicle. Its synthesis starts with multiple steps converting Acetyl-CoA to lanosterol. Thereafter two pathways exist: the Bloch pathway and Kandutsch-Russell pathway both produce cholesterol. Multiple genes from both pathways were expressed at lower levels in the FF cells derived from the high ΣDEHP group (Table 3A). Additionally, the low-density lipoprotein receptor (LDLR), essential for the import of cholesterol from circulating lipoproteins into cells (Miller and Bose, 2011), was downregulated in the high ΣDEHP group ($\log_2FC = -1.65$, FDR = 0.013), suggesting a potential disruption in cholesterol acquisition (Supplementary Table 4). Multiple DE miRNAs target the mRNAs of genes involved in both pathways as well as in the fatty acid biosynthesis pathway that uses cholesterol levels as a sensor

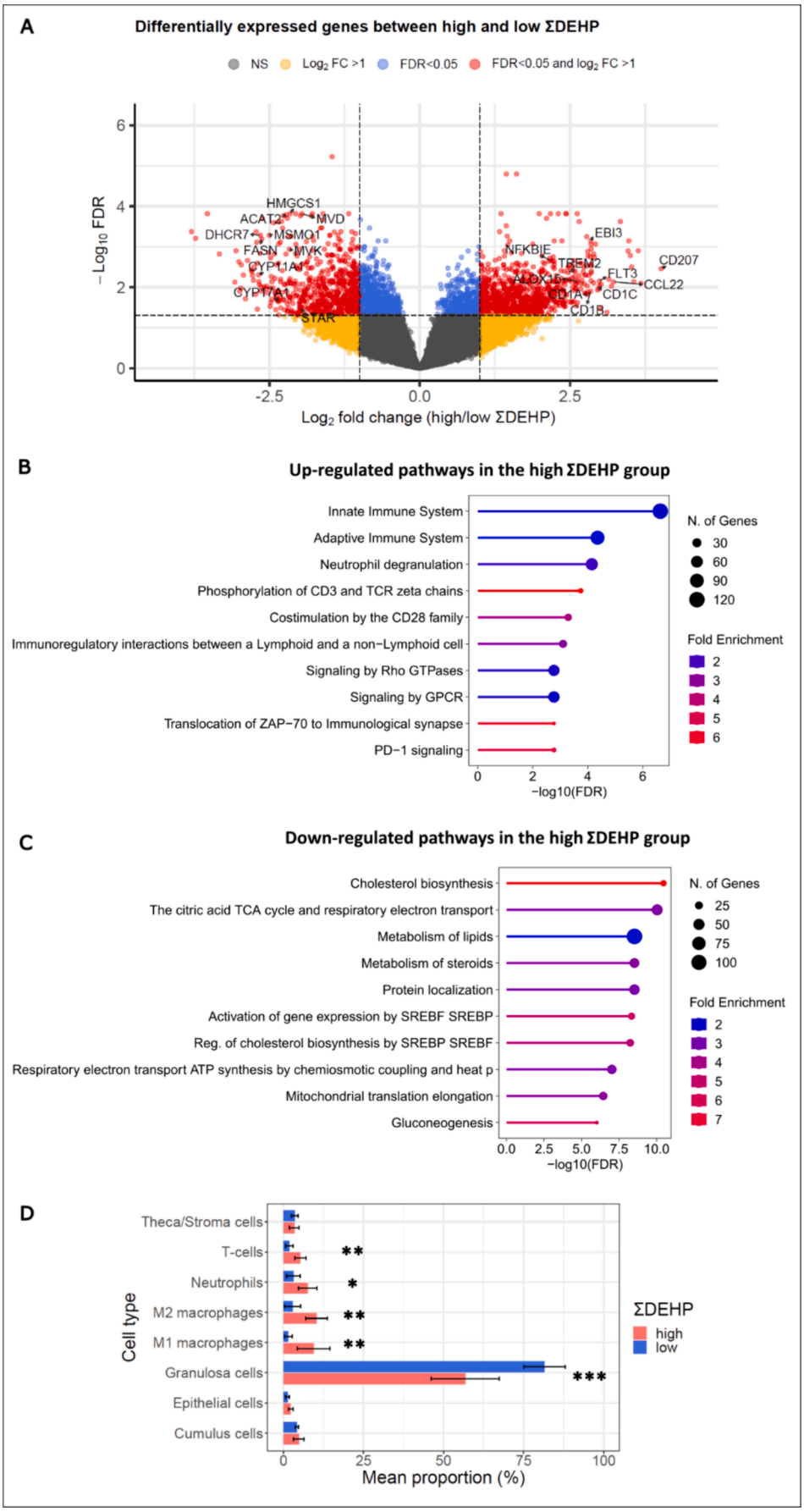

(caption on next page)

Fig. 2. Gene expression changes in the follicular fluid somatic cells in the high ΣDEHP group. A: Volcano plot depicting the distribution of differentially expressed genes in the high ΣDEHP group compared to low ΣDEHP group. B: Enriched Reactome pathways associated with upregulated genes in the high ΣDEHP group. C: Enriched Reactome pathways associated with downregulated genes in the high ΣDEHP group. D: Computationally predicted cell type proportions in the high and low ΣDEHP groups. Cell types according to Roos et al 2022. * $p < 0.05$, **$p < 0.01$, *** $p < 0.001$. NS – not significant, FC – fold change, FDR – false discovery rate.

Table 3
miRNA:mRNA interactions in the cholesterol metabolism (A) and steroidogenesis (B) pathways. Differentially expressed (DE) genes between high vs low ΣDEHP group (FDR < 0.05) and the corresponding DE miRNAs predicted to target them according to miRWalk are displayed. Text in brackets indicates the number of binding sites of the miRNA to the corresponding mRNA.

A Cholesterol metabolism

Gene symbol	log_2FoldChange	FDR	Targeting DE miRNA
MVD	−1.96	1.52E-04	none
HMGCS1	−2.16	1.52E-04	hsa-miR-150-5p, hsa-miR-205-5p (2x), hsa-miR28-3p (2x), hsa-miR-425-3p, hsa-miR-675-3p (2x)
ACAT2	−2.22	1.62E-04	none
FDPS	−2.27	1.72E-04	none
IDI1	−1.61	2.14E-04	hsa-miR-106b-3p, hsa-miR-122-5p, hsa-miR-203b-5p
FDFT1	−1.42	4.30E-04	none
MSMO1	−2.50	5.23E-04	hsa-miR-1307-5p (2x)
DHCR7	−2.65	5.23E-04	hsa-miR-199b-3p (2x), hsa-miR-425-3p
FASN	−2.63	6.43E-04	none
FADS1	−1.77	7.06E-04	hsa-miR-205-5p (2x), hsa-miR-4324
LSS	−2.32	7.65E-04	hsa-miR-106b-3p (3x), hsamiR-10b-5p (3x), hsa-miR-132-3p (3x)
SCD	−2.71	7.77E-04	none
MVK	−2.17	0.0011	hsa-miR-10b-5p (2x), hsa-miR-675-3p (2x)
SQLE	−2.00	0.0011	none
SC5D	−1.23	0.0015	hsa-miR-106b-3p
FADS2	−2.23	0.0015	hsa-miR-4324 (3x), hsa-miR-675-3p (3x)
CYP51A1	−2.04	0.0017	none
NSDHL	−1.87	0.0024	none
CYP27A1	2.66	0.0025	none
EBP	−1.95	0.0026	hsa-miR-122-5p
HMGCR	−1.45	0.0032	hsa-miR-4324 (4x)
HSD17B7	−1.13	0.0054	hsa-miR-675-3p
ELOVL5	−1.73	0.0063	hsa-miR-150-5p, hsa-miR-191-5p, hsa-miR-203b-5p, hsa-miR-28-3p (3x), hsa-miR-425-3p, hsa-miR-675-3p (2x)
SREBF1	−1.22	0.0085	hsa-miR-132-3p (3x), hsa-miR-199b-3p
PMVK	−0.83	0.0086	hsa-miR-205-5p
ABCG1	2.33	0.0110	hsa-miR-27a-3p, hsa-miR-4324 (2x), hsa-miR-106b-3p, hsa-miR-122-5p, hsa-miR-1307-5p, hsa-miR-191-5p

B Steroidogenesis

Gene symbol	log_2FoldChange	FDR	Targeting DE miRNA
CYP11A1/P450scc	−2.68	0.0049	none
CYB5A/cytochrome b5	−2.24	0.0087	hsa-miR-106-3p (2x), hsa-miR-132-3p, hsa-miR-27a-3p (2x), hsa-miR-675-3p
CYP17A1/P450c17	−2.34	0.0217	none
POR	−0.85	0.0342	none
STAR	−1.99	0.0348	hsa-miR-28-3p, hsa-miR-675-3p
CYP19A1/P450Aro	−1.62	0.0407	hsa-miR-132-3p (x2), hsa-miR-150-5p (x2), hsa-miR-199b-3p (x2), hsa-miR-205-5p (x3), hsa-miR-28-3p (x2)

(Ye and DeBose-Boyd, 2011) (Fig. 3A, Table 3A).

In the steroidogenesis pathway, the expression of *STAR* mRNAs, a transporter of cholesterol from the mitochondrial outer to the inner membrane (Miller, 2007) was lower in the high ΣDEHP group ($log_2FC = -1.99$, FDR = 0.035) (Table 3B). Additionally, the key steroidogenic enzymes *CYP11A1, CYP17A1* and *CYP19A1* as well as steroidogenesis regulators *POR* and *CYB5A* were all downregulated in the high ΣDEHP group (FDR < 0.05). Furthermore, we observed that *STAR*, *CYB5A* and *CYP19A1* are potential targets for the DE miRNAs present in the FF of the same follicles (Fig. 3B, Table 3B).

It must be emphasized that most miRNA-regulated mRNAs in Fig. 3 were predicted to be targeted by either multiple DE miRNAs or by miRNAs with multiple target sites on a particular mRNA sequence (Tables 3A and B) indicating strong targeting evidence (Sætrom et al., 2007).

3.5. Differences in the follicular fluid steroid levels between high and low ΣDEHP groups

Lastly, the concentrations of 12 steroid hormones were analyzed in the same FF samples with available ΣDEHP measurements and were compared between the high and low ΣDEHP groups adjusting for the country of origin. Although ASD and TES levels were lower in the high ΣDEHP group, the difference was not statistically significant ($p > 0.05$, Fig. 4A). To account for the individual variations in the FF steroid levels, we next considered the ratios between steroids as indicators of the associated enzyme activities. The analysis of the product-to-precursor ratios revealed that PRO to HPR ratio was lower in the high ΣDEHP group ($p = 0.046$, Fig. 4B). As mentioned above, the expression level of the mRNA of the enzyme in P450c17 (encoded by the *CYP17A1* gene) performing the conversion of PRO to HPR was 5 times lower in the follicular cells of the high ΣDEHP group ($log_2FC = -2.33$, FDR = 0.022, Fig. 3B, Supplementary Table 4).

4. Discussion

DEHP metabolites have been detected in human FF and linked to altered ovarian function: women with higher levels of 4 main DEHP metabolites (ΣDEHP) in their FF demonstrated diminished response to rFSH in COST (Bellavia et al., 2023). However, the underlying mechanisms for this association remain poorly understood. In this study, we sought to characterize the impact of ΣDEHP on the miRNA profile and

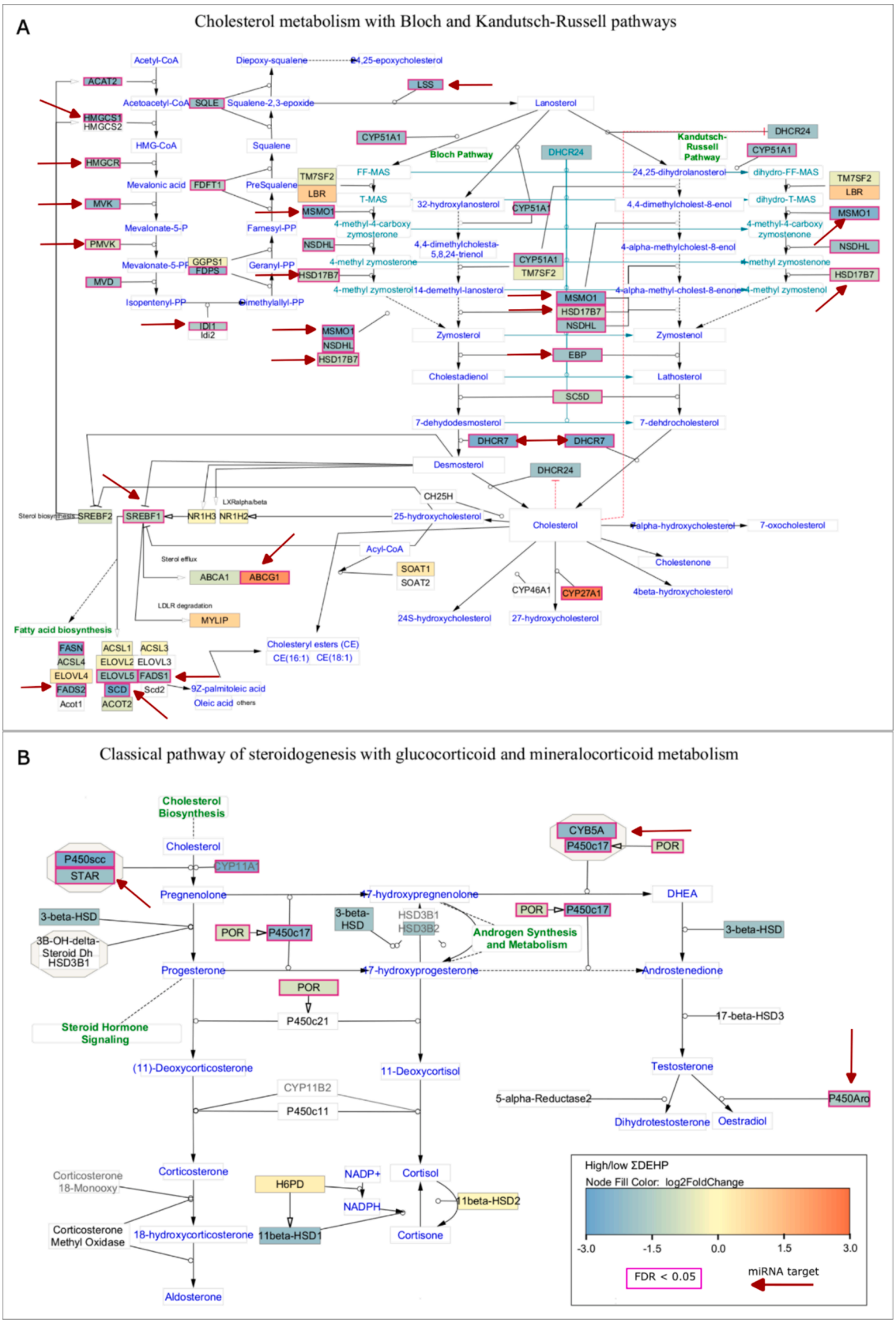

Fig. 3. Down-regulation of lipid and steroidogenesis synthesis pathways in the high ΣDEHP group. A: Cholesterol metabolism with Bloch and Kandutsch-Russell pathways; B: Classical pathway of steroidogenesis with glucocorticoid and mineralocorticoid metabolism. Gene expression fold differences are color-coded as depicted in the legend: blue colors refer to lower expression in the high ΣDEHP group. Differentially expressed (DE) genes between high and low ΣDEHP groups (FDR < 0.05) are highlighted with violet boxes. Genes predicted to be targeted by DE miRNAs are noted by red arrows. (For interpretation of the references to color in this figure legend, the reader is referred to the web version of this article.)

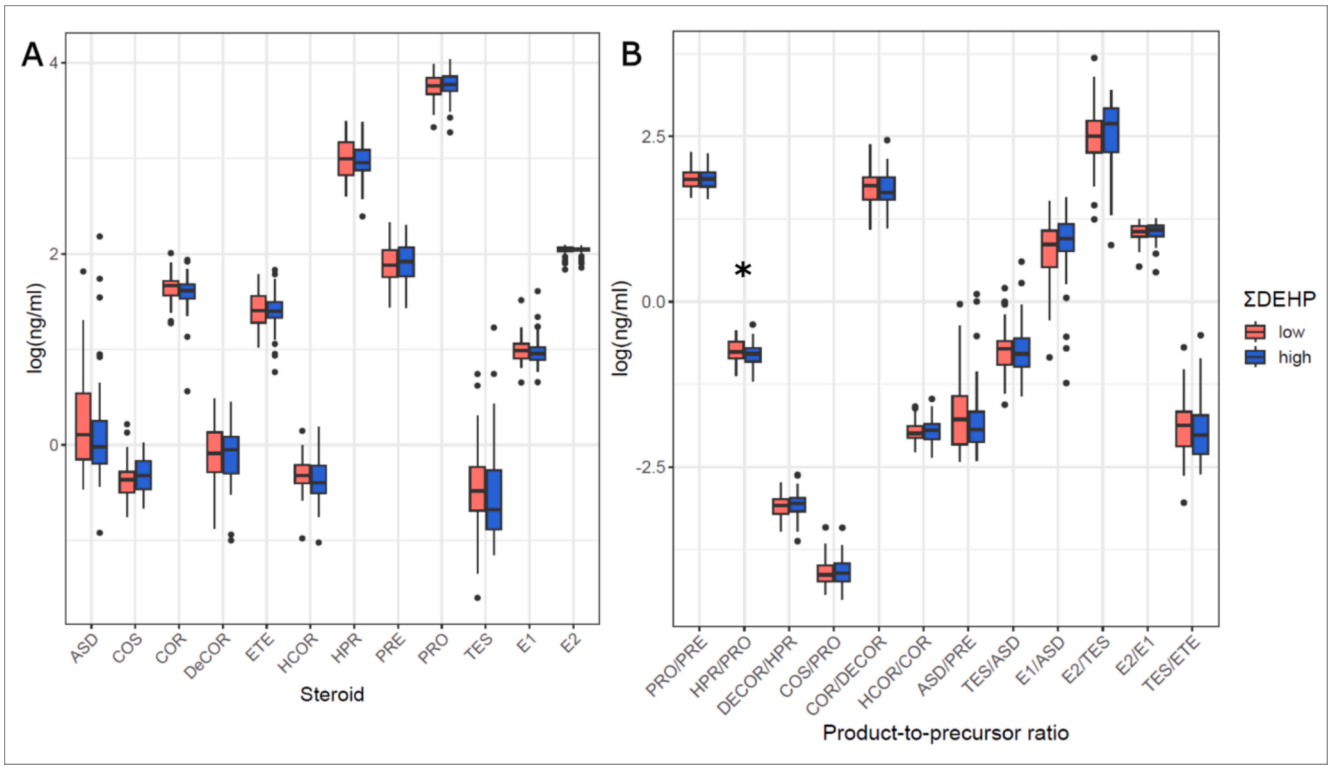

Fig. 4. Differences in the steroid hormone levels in the follicular fluid of women from low and high ΣDEHP groups. A: Steroid hormone levels; B: Product-to-precursor ratios of detected steroids. * p = 0.046, Welch's *t*-test adjusted for the country. ASD – androstenedione, COS – corticosterone, COR, cortisol, DeCOR – deoxycortisol, ETE – epi-testosterone, HCOR – hydroxycortisol, HPR – 17a-OH-progesterone, PRE – pregnenolone, PRO – progesterone, TES – testosterone, E1 – estrone, E2 – 17-β-estradiol.

the levels of steroid hormones of FF, as well as on mRNA expression in granulosa cells. To our knowledge, this is the first human cohort-based study to investigate the impact of the presence of ΣDEHP in follicles on human granulosa cell transcriptome and steroidogenesis, and to link the results with extracellular miRNA levels in the FF. Importantly, all measurements were performed from the same follicles, which allowed us to better scrutinize potential associations between different layers of information.

Our study presents compelling evidence for ΣDEHP-associated alterations in extracellular miRNA levels within FF. A total of 465 miRNAs were identified, 16 of which exhibited differential expression between high and low ΣDEHP groups. Changes in ovarian miRNA expression due to DEHP exposure have been observed in several animal studies (Liu et al., 2018; Patiño-García et al., 2020; Zhang et al., 2019). Culturing neonatal rodent ovaries with DEHP upregulates miR-28a-3p (Zhang et al., 2019), which suggests a causal connection between DEHP exposure and miRNA expression. Similarly, we observed an upregulation of miR-28a-3p in human FF in the presence of high ΣDEHP. Such an analogous response could suggest that miR-28a-3p modulation occurs across various organisms in response to DEHP, thus indicating a common molecular mechanism. While studies exploring the changes in miRNA profiles related to increased DEHP levels in human ovaries are limited, a negative correlation between urinary MEHP levels and miR-106b expression in FF extracellular vesicles (EV) has been reported (Martinez et al., 2019). In line with this, we observed a downregulation of miR-106b-3p in the FF of the high ΣDEHP group. However, another study exploring the association between FF phthalate concentration and EV miRNA expression did not find overlapping miRNAs with our study (Barnett-Itzhaki et al., 2021). This can be explained by partly distinct profiles between the cell-free and EV-packed miRNA sequences (Rooda et al., 2020). Secondly, the measured phthalate metabolites were different from those of our study. In addition, the absence of common miRNAs may be attributed to differences in patient cohorts, inclusion criteria, material collection and stimulation protocols as well as geographical differences in EDC exposure.

Our study revealed DE miRNAs associated with various reproductive conditions. Specifically, the upregulation of miR-27a-3p, miR-28a-3p, miR-122-5p and miR-199b-3p, and downregulation of miR-1307 in the high ΣDEHP group align with the expression patterns observed in patients with diminished ovarian reserve (Rapani et al., 2021; Xie et al., 2024). Additionally, the expression patterns of miR-122-5p and miR-132-3p in ovarian exosomes of mice with primary ovarian insufficiency was mirrored in our observations from the FF of the high ΣDEHP group (Zhang et al., 2022). A downregulation of miR-132-3p in FF has been linked with the generation of low-quality IVF embryos (Feng et al., 2015; Machtinger et al., 2017). The upregulation of miR-122-5p and miR-10b-5p, known to induce human granulosa cell apoptosis (Jiajie et al., 2017; Zhang et al., 2022), indicates that high ΣDEHP levels may contribute to altered granulosa cell dynamics. The upregulation of miR-203a-3p, previously observed in MII oocytes in older women and considered an indication for ovarian aging (Battaglia et al., 2016), is striking. Our results not only confirm the upregulation of miR-203a-3p in the high ΣDEHP group but also reveal a negative correlation with the OSI. This is noteworthy as decreased ovarian sensitivity is widely recognized as an indication of ovarian aging, and as a predictor for worse outcome in IVF treatments (Weghofer et al., 2020). Our findings thus suggest the possibility that ΣDEHP, by altering miR-203a-3p levels, may accelerate ovarian aging, contributing to the observed decline in ovarian sensitivity.

One of the mechanisms by which ΣDEHP may increase ovarian aging is by affecting AR signaling. Computational structural binding analysis suggests that DEHP metabolites have the potential to disrupt the AR function, as these metabolites closely resemble TES (Beg and Sheikh, 2020). However, direct binding of the DEHP metabolite MEHP has not

been confirmed in either yeast AR assays (Kim et al., 2019) nor in the human AR *in vitro* binding tests, even at supraphysiological concentrations (Parks et al., 2000). Our data shows that 6 of the DE miRNAs between the high and low ΣDEHP group target the AR signaling pathway that, in addition to the receptor, involves a plethora of AR-dependent transcription co-factors. The importance for AR signaling in the ovary has been established in model organisms and monogenic disorders (Panagiotou et al., 2022). The granulosa cell-specific AR knock-out mouse exhibits the signs of premature ovarian failure leading to subfertility (Sen and Hammes, 2010). Women suffering from androgen insensitivity syndrome-like monogenic disorders also exhibit poor ovarian response to gonadotrophins (Lissaman et al., 2023). Therefore, the potential disruption of AR signaling by ΣDEHP via miRNAs could have adverse consequences for the follicular development and function.

Molecular pathway enrichment analysis of DE miRNAs in FF revealed their involvement in adipogenesis, AGE/RAGE and RAC1/PAK1/p38/MMP2 pathways. Notably, rodent studies have demonstrated that DEHP acts as an obesogen, causing a substantial increase in body weight, food intake, and visceral adipose tissue compared to controls (Schmidt et al., 2012). These findings have been further supported by human studies, establishing an association between DEHP metabolites and obesity in adult females (Buser et al., 2014). The impact of DEHP and its metabolites on adipogenesis primarily occurs through the activation of peroxisome proliferator-activated receptors (PPARs) (Feige et al., 2007). Despite the absence of adipocytes in the ovarian follicle, the dysregulation of miRNAs targeting adipogenesis may signify potential alterations in fatty acid metabolism. Indeed, our results from RNA-seq of granulosa cells revealed the enrichment of downregulated genes in lipid and fatty acid metabolism pathways. Therefore, we hypothesize that differentially regulated miRNAs in the ovaries with high ΣDEHP levels could contribute to disturbances in fatty acid metabolism by targeting several genes, such as *FADS1, FADS2* and *SC5D*, within this pathway.

Advanced glycation end products (AGEs) are highly reactive molecules formed through lipid and protein glycation which exert their effects via receptor RAGEs. The accumulation of AGEs into the ovarian follicle has been proposed to trigger premature ovarian aging by promoting pro-inflammatory conditions (Tatone et al., 2008). Treatment of human cumulus cells with glycated albumin (a precursor for AGEs) has been shown to induce the expression of key steroidogenic genes (*CYP11A1, 3-βHSD, STAR, CYP17A1* and *LHR*), highlighting the pivotal role of AGEs in regulating steroidogenesis (Merhi, 2014). We hypothesize that dysregulation of the AGE/RAGE pathway through miRNAs in granulosa cells could be one of the mechanisms by which ΣDEHP alters the expression of steroidogenic enzymes and induces a pro-inflammatory environment within the follicle.

While the involvement of the RAC1/PAK1/p38/MMP2 pathway in normal ovarian function is not well-established, its implication in ovarian cancer is noteworthy (Gonzalez-Villasana et al., 2015). Matrix metalloproteinases, including MMP2, play crucial roles in follicle formation and rupture (Vos et al., 2014). Therefore, any disruptions in this signaling pathway that lead to MMP2 dysregulation could prove detrimental to these essential ovarian processes.

We identified 2,454 DE genes in granulosa cells between high and low ΣDEHP groups. Particularly interesting is the observation that the upregulated genes in high ΣDEHP follicles predominantly belong to immune system pathways. This finding is further substantiated by cellular deconvolution of our RNA-seq data, which revealed an increased presence of T-cells, neutrophils and macrophage markers within the ovarian follicle. This provides a potential explanation for the observed immune system related gene expression changes. These results also align with previous findings demonstrating the upregulation of immune response-associated genes in the ovaries of prepubertal mice exposed to DEHP (Lai et al., 2017). Moreover, phthalate metabolites or their mixtures have been shown to alter inflammatory cytokine levels in human FF (Wang et al., 2023). The enhanced presence of immune cells may indicate increased inflammation within the ovarian follicles, potentially compromising the microenvironment essential for successful ovulation. While further research is needed to clarify the immune mechanisms integral to ovarian function, our findings suggest that higher ΣDEHP levels may influence these processes.

Regulation of ovarian steroidogenesis is vital for the normal development and function of the ovarian follicles. In our study, higher concentration of ΣDEHP was associated with the reduced mRNA levels of genes encoding essential components of the steroidogenic pathway, including *CYP11A1, CYP17A1, CYP19A1* and *STAR*. Similar results have been observed in rodent studies, where *CYP17A1* and *STAR* were downregulated in rodent ovaries, and *CYP11A1, CYP19A1* and *STAR* expression levels were inhibited in rat granulosa cells upon DEHP exposure, accompanied by lower levels of PRO and estradiol in both studies (Lai et al., 2017; Tripathi et al., 2019). Our results also agree with experiments performed using primary human granulosa cells (Jin et al., 2019), cumulus cells (Tesic et al., 2023) and the granulosa-like tumor cell-line KGN (Jin et al., 2019). In these studies, DEHP decreased the expression of the same key steroidogenic enzymes (Guerra et al., 2016) accompanied by reduced PRO and estradiol production (Guerra et al., 2016; Tesic et al., 2023). Additionally, DEHP has been associated with reduced PRO levels in human FF (Du et al., 2019). Although we did not observe significant changes in FF steroid hormone levels between high and low ΣDEHP groups, we observed an altered ratio between PRO and HPR, which could be attributed to lower *CYP17A1* mRNA levels in the ovarian somatic cells of the high ΣDEHP group. Considering the predominantly luteinized state of the studied somatic cells, alterations in PRO conversion could negatively affect the developing corpus luteum and the maintenance of pregnancy. HPR serves as a precursor for ASD and cortisol production (Chakraborty et al., 2021; Honour, 2014), suggesting a potential influence on the synthesis of these hormones. Although a trend toward lower ASD and TES levels was observed between the study groups, we cannot confirm that the main mechanism of ΣDEHP action in the adult ovary is the inhibition of androgen synthesis as has been described for the testis (Desdoits-Lethimonier et al., 2012; Parks et al., 2000). Instead, our findings propose that *CYP19A1* and *STAR* mRNAs are targeted by multiple DE FF miRNAs, and the expression of *CYP17A1* is significantly reduced in the ovaries with high ΣDEHP. These results are indicative of decreased PRO metabolism.

Our transcriptional analyses revealed downregulation of 17 key genes involved in cholesterol, lipid and fatty acid metabolism pathways. mRNAs of 11 of these genes are potentially targeted by the DE FF miRNAs. Furthermore, considering that granulosa cells predominantly rely on cholesterol import from circulating lipoproteins (Miller and Bose, 2011), the downregulation of *LDLR* implies a potential imbalance in cellular cholesterol homeostasis. Given that cholesterol serves as a crucial precursor for the synthesis of steroid hormones, this downregulation could explain the observed decrease in steroidogenesis-related genes. Notably, the reduction in the expression of cholesterol metabolism genes *IDI1, FDFT1, CYP51A1* and *STARD1* has been implicated in granulosa cells of individuals with diminished ovarian reserve (Yang et al., 2022). Downregulation of genes involved in lipid and fatty acid metabolism could be detrimental for the maintenance of energy supplies in the granulosa cells (Zhang et al., 2023). Reduced utilization of fatty acids can lead to their accumulation in granulosa cells which can induce ovarian inflammation (Lai et al., 2022). This collective evidence strengthens the growing body of evidence connecting ΣDEHP to disruptions in ovarian function.

As a limitation of the current study we acknowledge that using samples from two heterogeneous populations might lead to fewer statistically significant results. Population heterogeneity can be attributed to differences not only in individual lifestyles, potentially influencing EDC levels, but also in stimulation protocols and sample collection routines between the clinics. However, this aspect effectively demonstrates the complexity of human studies and explains the frequent

discordances between different papers. As a strength, the current study stresses the robustness of the presented results as these have been validated in two patient sub cohorts covering the expected variability between lifestyle and fertility treatment standards between IVF patients from different countries.

5. Conclusions

In summary, our comprehensive analysis - spanning cell-free miRNA, cellular mRNA expression and steroid hormone measurements - reveals that high ΣDEHP level in human FF is linked with disrupted cholesterol and steroid hormone biosynthesis, altered PRO to HPR ratio, as well as with a pro-inflammatory environment within the ovarian follicle. Notably, some of these perturbations can be attributed to interrupted inter-cellular molecular communication via extracellular miRNAs. Our study suggests different mechanisms of action for ΣDEHP disruption in the adult ovaries to what has been previously described in the testis. This further demonstrates that EDCs such as ΣDEHP may have multiple mechanisms of action contributing to adverse outcomes, including in the ovaries. Overall, many of the changes reported here are associated with ovarian aging in other studies, indicating that EDCs like DEHP may accelerate reproductive senescence. There are still unresolved issues that warrant further scrutiny based on our findings, not least investigating in more detail how lipid metabolism, steroidogenesis, and inflammation is affected by ΣDEHP exposure in ovaries. However, our findings help explain the impact of EDC exposure on increasing female fertility problems.

Funding

This project has received funding from the European Union's Horizon 2020 research and innovation program under grant agreement No 825100 (FREIA), the Estonian Research Council (grants No. PSG608 and PRG1076), Horizon Europe (NESTOR, grant No. 101120075) of the European Commission, and FORMAS (Swedish Research Council for Environment, Agricultural Sciences and Spatial Planning, Grant No. 942-2015-476, 2015-00623, and 2018-02280).

Declaration of generative AI and AI-assisted technologies in the writing process

During the preparation of this work the authors used Microsoft Copilot in order to improve wording and correct grammar. After using this tool, the authors reviewed and edited the content as needed and take full responsibility for the content of the published article.

CRediT authorship contribution statement

Inge Varik: Writing – original draft, Visualization, Formal analysis. **Runyu Zou:** Writing – original draft, Visualization, Methodology, Formal analysis. **Andrea Bellavia:** Writing – review & editing, Methodology. **Kristine Rosenberg:** Writing – review & editing, Resources, Data curation. **Ylva Sjunnesson:** Writing – review & editing, Resources. **Ida Hallberg:** Writing – review & editing, Resources. **Jan Holte:** Resources. **Virissa Lenters:** Writing – review & editing, Methodology. **Majorie Van Duursen:** Writing – review & editing, Funding acquisition, Conceptualization. **Mikael Pedersen:** Methodology, Investigation, Formal analysis. **Terje Svingen:** Writing – review & editing. **Roel Vermeulen:** Writing – review & editing. **Andres Salumets:** Writing – review & editing, Funding acquisition. **Pauliina Damdimopoulou:** Writing – original draft, Supervision, Project administration, Conceptualization. **Agne Velthut-Meikas:** Writing – original draft, Visualization, Supervision, Investigation, Funding acquisition, Formal analysis, Data curation, Conceptualization.

Declaration of competing interest

The authors declare that they have no known competing financial interests or personal relationships that could have appeared to influence the work reported in this paper.

Data availability

The raw sequencing data files have been published in the European Nucleotide Archive under project number PRJEB74279.

Acknowledgments

We are grateful to the staff of Carl von Linnékliniken and Nova Vita Clinic for recruiting patients and all the study participants for donating their samples for research. We thank Dr. Lützen Portengen for his assistance in statistical analyses.

Appendix A. Supplementary material

Supplementary data to this article can be found online at https://doi.org/10.1016/j.envint.2024.108960.

References

Agrawal, A., Balcı, H., Hanspers, K., Coort, S.L., Martens, M., Slenter, D.N., et al., 2024. WikiPathways 2024: next generation pathway database. Nucleic Acids Res. 52, D679–D689. https://doi.org/10.1093/NAR/GKAD960.

Anders, S., Pyl, P.T., Huber, W., 2015. HTSeq–a Python framework to work with high-throughput sequencing data. Bioinformatics 31, 166–169. https://doi.org/10.1093/BIOINFORMATICS/BTU638.

Andersen, C., Krais, A.M., Eriksson, A.C., Jakobsson, J., Löndahl, J., Nielsen, J., et al., 2018. Inhalation and dermal uptake of particle and gas-phase phthalates—A human exposure study. Environ. Sci. Tech. 52, 12792–12800. https://doi.org/10.1021/acs.est.8b03761.

Aparicio-Puerta, E., Hirsch, P., Schmartz, G.P., Kern, F., Fehlmann, T., Keller, A., 2023. miEAA 2023: updates, new functional microRNA sets and improved enrichment visualizations. Nucleic Acids Res. 51, W319–W325. https://doi.org/10.1093/NAR/GKAD392.

Barnett-Itzhaki, Z., Knapp, S., Avraham, C., Racowsky, C., Hauser, R., Bollati, V., et al., 2021. Association between follicular fluid phthalate concentrations and extracellular vesicle microRNAs expression. Hum. Reprod. 36, 1590–1599. https://doi.org/10.1093/humrep/deab063.

Basso, C.G., de Araújo-Ramos, A.T., Martino-Andrade, A.J., 2022. Exposure to phthalates and female reproductive health: a literature review. Reprod. Toxicol. 109, 61–79. https://doi.org/10.1016/j.reprotox.2022.02.006.

Battaglia, R., Vento, M.E., Ragusa, M., Barbagallo, D., La Ferlita, A., Di Emidio, G., et al., 2016. MicroRNAs are stored in human MII oocyte and their expression profile changes in reproductive aging. Biol. Reprod. 95, 131. https://doi.org/10.1095/biolreprod.116.142711.

Beg, M.A., Sheikh, I.A., 2020. Endocrine disruption: structural interactions of androgen receptor against Di(2-ethylhexyl) phthalate and its metabolites. Toxics 8, 115. https://doi.org/10.3390/toxics8040115.

Bellavia, A., Zou, R., Björvang, R.D., Roos, K., Sjunnesson, Y., Hallberg, I., et al., 2023. Association between chemical mixtures and female fertility in women undergoing assisted reproduction in Sweden and Estonia. Environ. Res. 216, 114447 https://doi.org/10.1016/j.envres.2022.114447.

Bolger, A.M., Lohse, M., Usadel, B., 2014. Trimmomatic: a flexible trimmer for Illumina sequence data. Bioinformatics 30, 2114–2120. https://doi.org/10.1093/BIOINFORMATICS/BTU170.

Buser, M.C., Murray, H.E., Scinicariello, F., 2014. Age and sex differences in childhood and adulthood obesity association with phthalates: analyses of NHANES 2007–2010. Int. J. Hyg. Environ. Health 217, 687–694. https://doi.org/10.1016/j.ijheh.2014.02.005.

Chakraborty, S., Pramanik, J., Mahata, B., 2021. Revisiting steroidogenesis and its role in immune regulation with the advanced tools and technologies. Genes Immun. 22, 125–140. https://doi.org/10.1038/s41435-021-00139-3.

David, R.M., Bachman, A.N., Butala, J.H., Piper, J.T., Shelp, C.J., 2012. Esters of mono-, di-, and tricarboxylic acids. Patty's Toxicol. John Wiley & Sons, Ltd 147–352.

Desdoits-Lethimonier, C., Albert, O., Le Bizec, B., Perdu, E., Zalko, D., Courant, F., et al., 2012. Human testis steroidogenesis is inhibited by phthalates. Hum. Reprod. 27, 1451–1459. https://doi.org/10.1093/HUMREP/DES069.

Dobin, A., Davis, C.A., Schlesinger, F., Drenkow, J., Zaleski, C., Jha, S., et al., 2013. STAR: ultrafast universal RNA-seq aligner. Bioinformatics 29, 15–21. https://doi.org/10.1093/BIOINFORMATICS/BTS635.

Draskau, M.K., Boberg, J., Taxvig, C., Pedersen, M., Frandsen, H.L., Christiansen, S., et al., 2019. In vitro and in vivo endocrine disrupting effects of the azole fungicides

triticonazole and flusilazole. Environ. Pollut. 255. https://doi.org/10.1016/J.ENVPOL.2019.113309.
Du, Y., Guo, N., Wang, Y., Teng, X., Hua, X., Deng, T., et al., 2019. Follicular fluid concentrations of phthalate metabolites are associated with altered intrafollicular reproductive hormones in women undergoing in vitro fertilization. Fertil. Steril. 111, 953–961. https://doi.org/10.1016/j.fertnstert.2019.01.021.
European Chemicals Agency, 2024. Phthalates. https://echa.europa.eu/hot-topics/phthalates.
Feige, J.N., Gelman, L., Rossi, D., Zoete, V., Métivier, R., Tudor, C., et al., 2007. The endocrine disruptor monoethyl-hexyl-phthalate is a selective peroxisome proliferator-activated receptor gamma modulator that promotes adipogenesis. J. Biol. Chem. 282, 19152–19166. https://doi.org/10.1074/jbc.M702724200.
Feng, R., Sang, Q., Zhu, Y., Fu, W., Liu, M., Yan, Xu., et al., 2015. MiRNA-320 in the human follicular fluid is associated with embryo quality in vivo and affects mouse embryonic development in vitro. Sci. Rep. 5, 8689. https://doi.org/10.1038/srep08689.
Frederiksen, H., Jørgensen, N., Andersson, A.-M., 2010. Correlations between phthalate metabolites in urine, serum, and seminal plasma from young Danish men determined by isotope dilution liquid chromatography tandem mass spectrometry. J. Anal. Toxicol. 34, 400–410. https://doi.org/10.1093/jat/34.7.400.
Ge, S.X., Jung, D., Jung, D., Yao, R., 2020. ShinyGO: a graphical gene-set enrichment tool for animals and plants. Bioinformatics 36, 2628–2629. https://doi.org/10.1093/BIOINFORMATICS/BTZ931.
Gonzalez-Villasana, V., Fuentes-Mattei, E., Ivan, C., Dalton, H.J., Rodriguez-Aguayo, C., Fernandez-de Thomas, R.J., et al., 2015. Rac1/Pak1/p38/MMP-2 axis regulates angiogenesis in ovarian cancer. Clin. Cancer Res. 21, 2127–2137. https://doi.org/10.1158/1078-0432.CCR-14-2279.
Guerra, M.T., Furlong, H.C., Kempinas, W.G., Foster, W.G., 2016. Effects of in vitro exposure to butylparaben and di-(2 ethylhexyl) phthalate, alone or in combination, on ovarian function. J Appl. Toxicol. JAT 36, 1235–1245. https://doi.org/10.1002/jat.3335.
Hannon, P.R., Akin, J.W., Curry, T.E., 2023. Exposure to a phthalate mixture disrupts ovulatory progesterone receptor signaling in human granulosa cells in vitro†. Biol. Reprod. 109, 552–565. https://doi.org/10.1093/biolre/ioad091.
Hauser, R., Gaskins, A.J., Souter, I., Smith, K.W., Dodge, L.E., Ehrlich, S., et al., 2016. Urinary Phthalate Metabolite Concentrations and Reproductive Outcomes among Women Undergoing in Vitro Fertilization: Results from the EARTH Study. Environ. Health Perspect. 124, 831–839. https://doi.org/10.1289/ehp.1509760.
Högberg, J., Hanberg, A., Berglund, M., Skerfving, S., Remberger, M., Calafat, A.M., et al., 2008. Phthalate diesters and their metabolites in human breast milk, blood or serum, and urine as biomarkers of exposure in vulnerable populations. Environ. Health Perspect. 116, 334–339. https://doi.org/10.1289/ehp.10788.
Honour, J.W., 2014. 17-Hydroxyprogesterone in children, adolescents and adults. Ann. Clin. Biochem. 51, 424–440. https://doi.org/10.1177/0004563214529748.
Huber, M., Hadziosmanovic, N., Berglund, L., Holte, J., 2013. Using the ovarian sensitivity index to define poor, normal, and high response after controlled ovarian hyperstimulation in the long gonadotropin-releasing hormone-agonist protocol: suggestions for a new principle to solve an old problem. Fertil. Steril. 100. https://doi.org/10.1016/J.FERTNSTERT.2013.06.049.
Jiajie, T., Yanzhou, Y., Hoi-Hung, A.C., Zi-Jiang, C., Wai-Yee, C., 2017. Conserved miR-10 family represses proliferation and induces apoptosis in ovarian granulosa cells. Sci. Rep. 7, 41304. https://doi.org/10.1038/srep41304.
Jin, Y., Zhang, Q., Pan, J.-X., Wang, F.-F., Qu, F., 2019. The effects of di(2-ethylhexyl) phthalate exposure in women with polycystic ovary syndrome undergoing in vitro fertilization. J. Int. Med. Res. 47, 6278–6293. https://doi.org/10.1177/0300060519876467.
Katsikantami, I., Tzatzarakis, M.N., Alegakis, A.K., Karzi, V., Hatzidaki, E., Stavroulaki, A., et al., 2020. Phthalate metabolites concentrations in amniotic fluid and maternal urine: cumulative exposure and risk assessment. Toxicol Reports 7, 529–538. https://doi.org/10.1016/j.toxrep.2020.04.008.
Kehl, T., Kern, F., Backes, C., Fehlmann, T., Stöckel, D., Meese, E., et al., 2020. miRPathDB 2.0: a novel release of the miRNA pathway dictionary database. Nucleic Acids Res. 48, D142–D147. https://doi.org/10.1093/NAR/GKZ1022.
Kim, D.-H., Park, C.G., Kim, S.H., Kim, Y.J., 2019. The effects of mono-(2-Ethylhexyl) phthalate (MEHP) on human estrogen receptor (hER) and androgen receptor (hAR) by YES/YAS in vitro assay. Molecules 24, 1558. https://doi.org/10.3390/molecules24081558.
Koch, H.M., Preuss, R., Angerer, J., 2006. Di(2-ethylhexyl)phthalate (DEHP): human metabolism and internal exposure– an update and latest results. Int. J. Androl. 29, 155–185. https://doi.org/10.1111/j.1365-2605.2005.00607.x.
Kolberg, L., Raudvere, U., Kuzmin, I., Adler, P., Vilo, J., Peterson, H., 2023. g: Profiler—interoperable web service for functional enrichment analysis and gene identifier mapping (2023 update). Nucleic Acids Res. 51, W207–W212. https://doi.org/10.1093/NAR/GKAD347.
Koniecki, D., Wang, R., Moody, R.P., Zhu, J., 2011. Phthalates in cosmetic and personal care products: concentrations and possible dermal exposure. Environ. Res. 111, 329–336. https://doi.org/10.1016/j.envres.2011.01.013.
Kozomara, A., Birgaoanu, M., Griffiths-Jones, S., 2019. miRBase: from microRNA sequences to function. Nucleic Acids Res. 47, D155–D162. https://doi.org/10.1093/NAR/GKY1141.
Lai, F.-N., Liu, J.-C., Li, L., Ma, J.-Y., Liu, X.-L., Liu, Y.-P., et al., 2017. Di (2-ethylhexyl) phthalate impairs steroidogenesis in ovarian follicular cells of prepuberal mice. Arch. Toxicol. 91, 1279–1292. https://doi.org/10.1007/s00204-016-1790-z.
Lai, Y., Ye, Z., Mu, L., Zhang, Y., Long, X., Zhang, C., et al., 2022. Elevated levels of follicular fatty acids induce ovarian inflammation via ERK1/2 and inflammasome activation in PCOS. J. Clin. Endocrinol. Metab. 107, 2307–2317. https://doi.org/10.1210/clinem/dgac281.
Lissaman, A.C., Girling, J.E., Cree, L.M., Campbell, R.E., Ponnampalam, A.P., 2023. Androgen signalling in the ovaries and endometrium. Mol. Hum. Reprod. 29 https://doi.org/10.1093/MOLEHR/GAAD017.
Liu, J., Wang, W., Zhu, J., Li, Y., Luo, L., Huang, Y., et al., 2018. Di(2-ethylhexyl) phthalate (DEHP) influences follicular development in mice between the weaning period and maturity by interfering with ovarian development factors and microRNAs. Environ. Toxicol. 33, 535–544. https://doi.org/10.1002/tox.22540.
Liu, J.-C., Xing, C.-H., Xu, Y., Pan, Z.-N., Zhang, H.-L., Zhang, Y., et al., 2021. DEHP exposure to lactating mice affects ovarian hormone production and antral follicle development of offspring. J. Hazard. Mater. 416, 125862 https://doi.org/10.1016/j.jhazmat.2021.125862.
Love, M.I., Huber, W., Anders, S., 2014. Moderated estimation of fold change and dispersion for RNA-seq data with DESeq2. Genome Biol. 15 https://doi.org/10.1186/S13059-014-0550-8.
Lu, Z., Zhang, C., Han, C., An, Q., Cheng, Y., Chen, Y., et al., 2019. Plasticizer Bis(2-ethylhexyl) phthalate causes meiosis defects and decreases fertilization ability of mouse oocytes in vivo. J. Agric. Food Chem. 67, 3459–3468. https://doi.org/10.1021/acs.jafc.9b00121.
Machtinger, R., Rodosthenous, R.S., Adir, M., Mansour, A., Racowsky, C., Baccarelli, A. A., et al., 2017. Extracellular microRNAs in follicular fluid and their potential association with oocyte fertilization and embryo quality: an exploratory study. J. Assist. Reprod. Genet. 34, 525–533. https://doi.org/10.1007/s10815-017-0876-8.
Machtinger, R., Gaskins, A.J., Racowsky, C., Mansur, A., Adir, M., Baccarelli, A.A., et al., 2018. Urinary concentrations of biomarkers of phthalates and phthalate alternatives and IVF outcomes. Environ. Int. 111, 23–31. https://doi.org/10.1016/j.envint.2017.11.011.
Martinez, R.M., Hauser, R., Liang, L., Mansur, A., Adir, M., Dioni, L., et al., 2019. Urinary concentrations of phenols and phthalate metabolites reflect extracellular vesicle microRNA expression in follicular fluid. Environ. Int. 123, 20–28. https://doi.org/10.1016/j.envint.2018.11.043.
Merhi, Z., 2014. Advanced glycation end products and their relevance in female reproduction. Hum. Reprod. 29, 135–145. https://doi.org/10.1093/humrep/det383.
Messerlian, C., Souter, I., Gaskins, A.J., Williams, P.L., Ford, J.B., Chiu, Y.-H., et al., 2016. Urinary phthalate metabolites and ovarian reserve among women seeking infertility care. Hum. Reprod. 31, 75–83. https://doi.org/10.1093/humrep/dev292.
Miller, W.L., 2007. Steroidogenic acute regulatory protein (StAR), a novel mitochondrial cholesterol transporter. Biochim. Biophys. Acta 1771, 663–676. https://doi.org/10.1016/J.BBALIP.2007.02.012.
Miller, W.L., Bose, H.S., 2011. Early steps in steroidogenesis: intracellular cholesterol trafficking. J. Lipid Res. 52, 2111–2135. https://doi.org/10.1194/JLR.R016675.
Muczynski, V., Lecureuil, C., Messiaen, S., Guerquin, M.-J., N'tumba-Byn, T., Moison, D., et al., 2012. Cellular and molecular effect of MEHP Involving LXRα in human fetal testis and ovary. PLoS One 7, e48266. https://doi.org/10.1371/journal.pone.0048266.
Newman, A.M., Steen, C.B., Liu, C.L., Gentles, A.J., Chaudhuri, A.A., Scherer, F., et al., 2019. Determining cell type abundance and expression from bulk tissues with digital cytometry. Nat. Biotechnol. 37, 773–782. https://doi.org/10.1038/S41587-019-0114-2.
Panagiotou, E.M., Draskau, M.K., Li, T., Hirschberg, A., Svingen, T., Damdimopoulou, P., 2022. AOP key event relationship report: Linking decreased androgen receptor activation with decreased granulosa cell proliferation of gonadotropin-independent follicles. Reprod. Toxicol. 112, 136–147. https://doi.org/10.1016/J.REPROTOX.2022.07.004.
Paoli, D., Pallotti, F., Dima, A.P., Albani, E., Alviggi, C., Causio, F., et al., 2020. Phthalates and bisphenol A: presence in blood serum and follicular fluid of italian women undergoing assisted reproduction techniques. Toxics 8, 91. https://doi.org/10.3390/toxics8040091.
Parks, L.G., Ostby, J.S., Lambright, C.R., Abbott, B.D., Klinefelter, G.R., Barlow, N.J., et al., 2000. The plasticizer diethylhexyl phthalate induces malformations by decreasing fetal testosterone synthesis during sexual differentiation in the male rat. Toxicol. Sci. An Off J. Soc. Toxicol. 58, 339–349. https://doi.org/10.1093/toxsci/58.2.339.
Patiño-García, D., Cruz-Fernandes, L., Buñay, J., Orellana, R., Moreno, R.D., 2020. Daily exposure to phthalates and alkylphenols alters miR biogenesis and expression in mice ovaries. J. Mol. Endocrinol. 65, 175–186. https://doi.org/10.1530/JME-20-0149.
Picelli, S., Faridani, O.R., Björklund, Å.K., Winberg, G., Sagasser, S., Sandberg, R., 2014. Full-length RNA-seq from single cells using Smart-seq2. Nat. Protoc. 9, 171–181. https://doi.org/10.1038/NPROT.2014.006.
R Core Team, 2023. No Title. R A Lang Environ Stat Comput R Found Stat Comput Vienna, Austria. https://www.r-project.org/.
Rapani, A., Nikiforaki, D., Karagkouni, D., Sfakianoudis, K., Tsioulou, P., Grigoriadis, S., et al., 2021. Reporting on the role of miRNAs and affected pathways on the molecular backbone of ovarian insufficiency: a systematic review and critical analysis mapping of future research. Front. Cell Dev. Biol. 8, 590106 https://doi.org/10.3389/FCELL.2020.590106/FULL.
Revelli, A., Gennarelli, G., Biasoni, V., Chiadò, A., Carosso, A., Evangelista, F., et al., 2020. The Ovarian Sensitivity Index (OSI) significantly correlates with ovarian reserve biomarkers, is more predictive of clinical pregnancy than the total number of oocytes, and is consistent in consecutive IVF cycles. J. Clin. Med. 9, 1–8. https://doi.org/10.3390/JCM9061914.
Rooda, I., Hasan, M.M., Roos, K., Viil, J., Andronowska, A., Smolander, O.-P., et al., 2020. Cellular, extracellular and extracellular vesicular miRNA profiles of pre-

ovulatory follicles indicate signaling disturbances in polycystic ovaries. Int. J. Mol. Sci. 21, 9550. https://doi.org/10.3390/ijms21249550.
Roos, K., Rooda, I., Keif, R.-S., Liivrand, M., Smolander, O.-P., Salumets, A., et al., 2022. Single-cell RNA-seq analysis and cell-cluster deconvolution of the human preovulatory follicular fluid cells provide insights into the pathophysiology of ovarian hyporesponse. Front. Endocrinol. (Lausanne) 13, 945347. https://doi.org/10.3389/fendo.2022.945347.
Sætrom, P., Heale, B.S.E., Snøve, O., Aagaard, L., Alluin, J., Rossi, J.J., 2007. Distance constraints between microRNA target sites dictate efficacy and cooperativity. Nucleic Acids Res. 35, 2333–2342. https://doi.org/10.1093/NAR/GKM133.
Schettler, T., 2006. Human exposure to phthalates via consumer products. Int. J. Androl. 29, 134–139. https://doi.org/10.1111/j.1365-2605.2005.00567.x.
Schmidt, J.-S., Schaedlich, K., Fiandanese, N., Pocar, P., Fischer, B., 2012. Effects of di(2-ethylhexyl) phthalate (DEHP) on female fertility and adipogenesis in C3H/N mice. Environ. Health Perspect. 120, 1123–1129. https://doi.org/10.1289/ehp.1104016.
Schug, T.T., Janesick, A., Blumberg, B., Heindel, J.J., 2011. Endocrine disrupting chemicals and disease susceptibility. J. Steroid Biochem. Mol. Biol. 127, 204–215. https://doi.org/10.1016/j.jsbmb.2011.08.007.
Sen, A., Hammes, S.R., 2010. Granulosa cell-specific androgen receptors are critical regulators of ovarian development and function. Mol. Endocrinol. 24, 1393–1403. https://doi.org/10.1210/ME.2010-0006.
Shannon, P., Markiel, A., Ozier, O., Baliga, N.S., Wang, J.T., Ramage, D., et al., 2003. Cytoscape: a software environment for integrated models of biomolecular interaction networks. Genome Res. 13, 2498–2504. https://doi.org/10.1101/GR.1239303.
Sticht, C., De La Torre, C., Parveen, A., Gretz, N., 2018. miRWalk: an online resource for prediction of microRNA binding sites. PLoS One 13, e0206239. https://doi.org/10.1371/JOURNAL.PONE.0206239.
Tatone, C., Amicarelli, F., Carbone, M.C., Monteleone, P., Caserta, D., Marci, R., et al., 2008. Cellular and molecular aspects of ovarian follicle ageing. Hum. Reprod. Update 14, 131–142. https://doi.org/10.1093/humupd/dmm048.
Tesic, B., Samardzija Nenadov, D., Tomanic, T., Fa Nedeljkovic, S., Milatovic, S., Stanic, B., et al., 2023. DEHP decreases steroidogenesis through the cAMP and ERK1/2 signaling pathways in FSH-stimulated human granulosa cells. Cells 12, 398. https://doi.org/10.3390/cells12030398.
Tripathi, A., Pandey, V., Sahu, A.N., Singh, A., Dubey, P.K., 2019. Di-(2-ethylhexyl) phthalate (DEHP) inhibits steroidogenesis and induces mitochondria-ROS mediated apoptosis in rat ovarian granulosa cells. Toxicol. Res. (Camb) 8, 381–394. https://doi.org/10.1039/c8tx00263k.
Vaegter, K.K., Berglund, L., Tilly, J., Hadziosmanovic, N., Brodin, T., Holte, J., 2019. Construction and validation of a prediction model to minimize twin rates at preserved high live birth rates after IVF. Reprod. Biomed. 38, 22–29. https://doi.org/10.1016/J.RBMO.2018.09.020.
Valadi, H., Ekström, K., Bossios, A., Sjöstrand, M., Lee, J.J., Lötvall, J.O., 2007. Exosome-mediated transfer of mRNAs and microRNAs is a novel mechanism of genetic exchange between cells. Nat. Cell Biol. 9, 654–659. https://doi.org/10.1038/NCB1596.
Vos, M.C., van der Wurff, A.A.M., Last, J.T.J., de Boed, E.A.M., Smeenk, J.M.J., van Kuppevelt, T.H., et al., 2014. Immunohistochemical expression of MMP-14 and MMP-2, and MMP-2 activity during human ovarian follicular development. Reprod. Biol. Endocrinol. 12, 12. https://doi.org/10.1186/1477-7827-12-12.
Wang, Y., Du, Y.-Y., Yao, W., Deng, T.-R., Guo, N., Yin, L., et al., 2023. Associations between phthalate metabolites and cytokines in the follicular fluid of women undergoing in vitro fertilization. Ecotoxicol. Environ. Saf. 267, 115616 https://doi.org/10.1016/j.ecoenv.2023.115616.
Weghofer, A., Barad, D.H., Darmon, S.K., Kushnir, V.A., Albertini, D.F., Gleicher, N., 2020. The ovarian sensitivity index is predictive of live birth chances after IVF in infertile patients. Hum. Reprod. Open 2020, hoaa049. https://doi.org/10.1093/HROPEN/HOAA049.
Xie, Y., Chen, J., Liu, K., Huang, J., Zeng, Y., Gao, M., et al., 2024. Differential expression of follicular fluid exosomal microRNA in women with diminished ovarian reserve. J. Assist. Reprod. Genet. https://doi.org/10.1007/S10815-024-03037-5.
Yang, X., Zhao, Z., Fan, Q., Li, H., Zhao, L., Liu, C., et al., 2022. Cholesterol metabolism is decreased in patients with diminished ovarian reserve. Reprod. Biomed. 44, 185–192. https://doi.org/10.1016/j.rbmo.2021.09.013.
Ye, J., DeBose-Boyd, R.A., 2011. Regulation of cholesterol and fatty acid synthesis. Cold Spring Harb. Perspect. Biol. 3, 1–13. https://doi.org/10.1101/CSHPERSPECT.A004754.
Zhang, C.-H., Liu, X.-Y., Wang, J., 2023. Essential role of granulosa cell glucose and lipid metabolism on oocytes and the potential metabolic imbalance in polycystic ovary syndrome. Int. J. Mol. Sci. 24, 16247. https://doi.org/10.3390/ijms242216247.
Zhang, J.-N., Zhang, R.-Q., Liu, J.-C., Li, L., Shen, W., Sun, X.-F., 2019. Di (2-ethylhexyl) phthalate exposure impairs the microRNAs expression profile during primordial follicle assembly. Front. Endocrinol. (Lausanne) 10, 877. https://doi.org/10.3389/fendo.2019.00877.
Zhang, X., Zhang, R., Hao, J., Huang, X., Liu, M., Lv, M., et al., 2022. miRNA-122-5p in POI ovarian-derived exosomes promotes granulosa cell apoptosis by regulating BCL9. Cancer Med. 11, 2414–2426. https://doi.org/10.1002/cam4.4615.